

Frank-Wolfe Bayesian Quadrature: Probabilistic Integration with Theoretical Guarantees

François-Xavier Briol
 Department of Statistics
 University of Warwick
 f-x.briol@warwick.ac.uk

Chris J. Oates
 School of Mathematical and Physical Sciences
 University of Technology, Sydney
 christopher.oates@uts.edu.au

Mark Girolami
 Department of Statistics
 University of Warwick
 m.girolami@warwick.ac.uk

Michael A. Osborne
 Department of Engineering Science
 University of Oxford
 mosb@robots.ox.ac.uk

Abstract

There is renewed interest in formulating integration as an inference problem, motivated by obtaining a full distribution over numerical error that can be propagated through subsequent computation. Current methods, such as Bayesian Quadrature, demonstrate impressive empirical performance but lack theoretical analysis. An important challenge is to reconcile these probabilistic integrators with rigorous convergence guarantees. In this paper, we present the first probabilistic integrator that admits such theoretical treatment, called Frank-Wolfe Bayesian Quadrature (FWBQ). Under FWBQ, convergence to the true value of the integral is shown to be exponential and posterior contraction rates are proven to be super-exponential. In simulations, FWBQ is competitive with state-of-the-art methods and out-performs alternatives based on Frank-Wolfe optimisation. Our approach is applied to successfully quantify numerical error in the solution to a challenging model choice problem in cellular biology.

1 Introduction

Computing integrals is a core challenge in machine learning and numerical methods play a central role. This can be problematic when a numerical integration routine is repeatedly called, maybe millions of times, within a larger computational pipeline. In such situations, the cumulative impact of numerical errors can be unclear, especially in cases where the error has a non-trivial structural component. One solution is to model the numerical error statistically and to propagate this source of uncertainty through subsequent computations. Conversely, an understanding of how errors arise and propagate can enable the efficient focusing of computational resources upon the most challenging numerical integrals in a pipeline.

Classical quadrature and cubature schemes do not account for prior information on the integrand and, as a consequence, can require an excessive number of function evaluations to obtain a prescribed level of accuracy [20]. Alternatives such as Quasi-Monte Carlo (QMC) can exploit knowledge on the smoothness of the integrand to obtain optimal convergence rates [6]. However these optimal rates can only hold on sub-sequences of sample sizes n , a consequence of the fact that all function evaluations are weighted equally in the estimator [23]. A modern approach that avoids this problem is to consider arbitrarily weighted combinations of function values; the so-called *sigma-point rules* [25]. Whilst

sigma-point rules have received comparatively little theoretical attention, it is known that the extra flexibility given by arbitrary weights can lead to extremely accurate approximations in many settings (see applications to image denoising [3] and mental simulation in psychology [12]).

Probabilistic numerics, introduced in the seminal paper of [5], aims at re-interpreting numerical tasks as inference tasks that are amenable to statistical analysis.¹ Recent developments include probabilistic solvers for linear systems [13] and differential equations [26]. For the task of computing integrals, Bayesian Quadrature (BQ) [21] and more recent work by [19] provide probabilistic numerics methods that produce a full posterior distribution on the output of numerical schemes. One advantage of this approach is that we can propagate uncertainty through all subsequent computations to explicitly model the impact of numerical error [14]. Contrast this with chaining together classical error bounds; the result in such cases will typically be a weak bound that provides no insight into the error structure. At present, a significant shortcoming of these methods is the absence of theoretical results relating to rates of posterior contraction. This is unsatisfying and has likely hindered the adoption of probabilistic approaches to integration, since it is not clear that the induced posteriors represent a sensible quantification of the numerical error (by classical, frequentist standards).

This paper establishes convergence rates for a new probabilistic approach to integration. Our results thus overcome a key perceived weakness associated with probabilistic numerics in the quadrature setting. Our starting point is recent work by [2], who cast the design of quadrature rules as a problem in convex optimisation that can be solved using the Frank-Wolfe (FW) algorithm. We propose a hybrid approach of [2] with BQ, taking the form of a sigma-point rule, that (i) carries a full probabilistic interpretation, (ii) is amenable to rigorous theoretical analysis, and (iii) converges orders-of-magnitude faster, empirically, compared with the original approaches in [2]. In particular, we prove that super-exponential rates hold for posterior contraction, showing that the posterior distribution provides a sensible and effective quantification of the uncertainty arising from numerical error. The methodology is explored in simulations and also applied to a challenging model selection problem from cellular biology, where numerical error could lead to mis-allocation of expensive resources.

2 Background

2.1 Quadrature and Cubature Methods

Let $\mathcal{X} \subseteq \mathbb{R}^d$ be a measurable space such that $d \in \mathbb{N}_+$ and consider a probability density $p(x)$ defined with respect to the Lebesgue measure on \mathcal{X} . This paper focuses on computing integrals of the form $\int f(x)p(x)dx$ for a test function $f : \mathcal{X} \rightarrow \mathbb{R}$ where, for simplicity, we assume f is square-integrable with respect to $p(x)$. A ‘sigma-point rule’ approximates such integrals as a weighted sum of function values at some design points $\{x_i\}_{i=1}^n \subset \mathcal{X}$:

$$\int f(x)p(x)dx \approx \sum_{i=1}^n w_i f(x_i). \quad (1)$$

Viewing integrals as projections, we write $p[f]$ for the left-hand side and $\hat{p}[f]$ for the right-hand side, where $\hat{p} = \sum_{i=1}^n w_i \delta(x_i)$ and $\delta(x_i)$ is a Dirac measure at x_i . Note that \hat{p} may not be a probability distribution; in fact, weights $\{w_i\}_{i=1}^n$ do not have to sum to one or be non-negative. Sigma-point rules can be extended to multivariate functions $f : \mathcal{X} \rightarrow \mathbb{R}^d$ by taking each component in turn.

There are many ways of choosing combinations $\{x_i, w_i\}_{i=1}^n$ in the literature. For example, taking weights to be $w_i = 1/n$ with points $\{x_i\}_{i=1}^n$ drawn independently from the probability distribution p recovers basic Monte Carlo integration. The case with weights $w_i = 1/n$, but with points chosen with respect to some specific (possibly deterministic) schemes includes Kernel Herding [4] and Quasi-Monte Carlo (QMC) [6]. In Bayesian Quadrature, the points $\{x_i\}_{i=1}^n$ are chosen to minimise a posterior variance, with weights $\{w_i\}_{i=1}^n$ arising from a posterior probability distribution.

¹A detailed discussion on probabilistic numerics and an extensive up-to-date bibliography can be found at <http://www.probablistic-numerics.org>.

Classical error analysis for sigma-point rules is naturally couched in terms of minimising the worst-case estimation error. Let \mathcal{H} be a Hilbert space of functions $f : \mathcal{X} \rightarrow \mathbb{R}$, equipped with the inner product $\langle \cdot, \cdot \rangle$ and associated norm $\| \cdot \|$. We define the maximum mean discrepancy (MMD) as:

$$\text{MMD}(\{x_i, w_i\}_{i=1}^n) := \sup_{f \in \mathcal{H}: \|f\|=1} \|p[f] - \hat{p}[f]\| \quad (2)$$

The reader can refer to [27] for conditions on \mathcal{H} that are needed for the existence of the MMD. The rate at which the MMD decreases with the number of samples n is referred to as the ‘convergence rate’ of the sigma-point rule. For Monte Carlo, the MMD decreases with the slow rate of $\mathcal{O}_P(n^{-1/2})$ (where the subscript P specifies that the convergence is in probability). Let \mathcal{H} be a RKHS with reproducing kernel $k : \mathcal{X} \times \mathcal{X} \rightarrow \mathbb{R}$ and denote the corresponding canonical feature map by $\Phi(x) = k(\cdot, x)$, so that the mean element is given $\mu_p(x) = p[\Phi(x)] \in \mathcal{H}$. Then, following [27]

$$\text{MMD}(\{x_i, w_i\}_{i=1}^n) = \|\mu_p - \mu_{\hat{p}}\|. \quad (3)$$

This shows that to obtain low integration error in the RKHS \mathcal{H} , one only needs to obtain a good approximation of its mean element μ_p (as $\forall f \in \mathcal{H}: p[f] = \langle f, \mu_p \rangle$). Establishing theoretical results for such quadrature rules is an active area of research [1].

2.2 Bayesian Quadrature

Bayesian Quadrature (BQ) was originally introduced in [21] and later revisited by [10, 11] and [22]. The main idea is to place a functional prior on the integrand f , then update this prior through Bayes’ theorem by conditioning on both samples $\{x_i\}_{i=1}^n$ and function evaluations at those sample points $\{f_i\}_{i=1}^n$ where $f_i = f(x_i)$. This induces a full posterior distribution over functions f and hence over the value of the integral $p[f]$. The most common implementation assumes a Gaussian Process (GP) prior $f \sim \mathcal{GP}(0, k)$. A useful property motivating the use of GPs is that linear projection preserves normality, so that the posterior distribution for the integral $p[f]$ is also a Gaussian, characterised by its mean and covariance. A natural estimate of the integral $p[f]$ is given by the mean of this posterior distribution, which can be compactly written as

$$\hat{p}_{\text{BQ}}[f] = \mathbf{z}^T K^{-1} \mathbf{f}. \quad (4)$$

where $z_i = \mu_p(x_i)$ and $K_{ij} = k(x_i, x_j)$. Notice that this estimator takes the form of a sigma-point rule with weights $w^{\text{BQ}} = \mathbf{z}^T K^{-1}$. This begs the question of how to select design points $\{x_i\}_{i=1}^n$. Recently, [25] showed how specific choices of kernel and design points can recover classical quadrature rules. A particularly natural approach aims to minimise the posterior uncertainty over the integral $p[f]$, which was shown in [Prop. 1, [15]] to equal:

$$v_{\text{BQ}}(\{x_i\}_{i=1}^n) = p[\mu_p] - \mathbf{z}^T K^{-1} \mathbf{z} = \text{MMD}(\{x_i, w_i^{\text{BQ}}\}_{i=1}^n)^2. \quad (5)$$

Thus, in the RKHS setting, minimising the posterior variance corresponds to minimising the worst case error of the sigma-point rule. Below we refer to Optimal BQ (OBQ) as BQ coupled with design points $\{x_i^{\text{OBQ}}\}_{i=1}^n$ chosen to globally minimise (5). We also call Sequential BQ (SBQ) the algorithm that greedily selects design points to give the greatest decrease in posterior variance at each iteration. OBQ will give improved results over SBQ, but cannot be implemented in general, whereas SBQ is comparatively straight-forward to implement. There are currently no theoretical results establishing the convergence of either BQ, OBQ or SBQ.

Remark: (5) is independent of observed function values \mathbf{f} . As such, no active learning is possible in SBQ (i.e. surprising function values never cause a revision of a planned sampling schedule). This is not the case for general sigma-point rules: For example [11] approximately encodes non-negativity of f into BQ and this leads to a dependence on \mathbf{f} in the posterior variance. In this case sequential selection becomes an *active* strategy that outperforms batch selection in general.

Algorithm 1 The Frank-Wolfe (FW) and Frank-Wolfe with Line-Search (FWLS) Algorithms.

Require: function J , initial state $g_0 \in \mathcal{G}$ (and, for FW only: step-size sequence $\{\rho_i\}_{i=1}^n$).

- 1: **for** $i = 0, \dots, n - 1$ **do**
 - 2: Compute $\bar{g}_i = \operatorname{argmin}_{g \in \mathcal{G}} \langle g, (DJ)(g_i) \rangle$
 - 3: [For FWLS only, line search: $\rho_i = \operatorname{argmin}_{\rho \in [0,1]} J((1 - \rho)g_i + \rho \bar{g}_i)$]
 - 4: Update $g_{i+1} = (1 - \rho_i)g_i + \rho_i \bar{g}_i$
 - 5: **end for**
-

2.3 Deriving Quadrature Rules via the Frank-Wolfe Algorithm

Despite the elegance of BQ, its convergence rates have not yet been rigorously established. In brief, this is because $\hat{p}_{\text{BQ}}[f]$ is an orthogonal projection of f onto the *affine* hull of $\{\Phi(x_i)\}_{i=1}^n$, rather than e.g. the *convex* hull. Standard results from the optimisation literature apply to bounded domains, but the affine hull is not bounded (i.e. the BQ weights can be arbitrarily large and possibly negative). Below we describe a solution recently proposed by [2], based on the FW algorithm, that restricts attention to the (bounded) convex hull of $\{\Phi(x_i)\}_{i=1}^n$.

The Frank-Wolfe (FW) algorithm (Alg. 1), also called the conditional gradient algorithm, is a convex optimization method introduced in [8]. It considers problems of the form $\min_{g \in \mathcal{G}} J(g)$ where the function $J : \mathcal{G} \rightarrow \mathbb{R}$ is convex and continuously differentiable. A particular case of interest in this paper will be when the domain \mathcal{G} is a compact and convex space of functions, as recently investigated in [16]. These assumptions imply the existence of a solution to the optimization problem.

Let $\mathcal{L}(\mathcal{A}, \mathcal{B})$ denote the space of bounded linear maps between Hilbert spaces \mathcal{A}, \mathcal{B} . In the quadrature setting, DJ denotes the Fréchet derivative of J , defined to be a map $DJ : \mathcal{H} \rightarrow \mathcal{L}(\mathcal{H}, \mathbb{R})$ such that, for each $g \in \mathcal{H}$, $(DJ)(g)$ is the function mapping $h \in \mathcal{H}$ to $(DJ)(g)(h) = \langle g - \mu_p, h \rangle \in \mathbb{R}$. At each iteration i , the FW algorithm computes a linearisation of the objective J at the current state $g_i \in \mathcal{G}$ along its gradient $(DJ)(g_i)$ and selects an ‘atom’ $\bar{g}_i \in \mathcal{G}$ that minimises this linearisation. The new state $g_{i+1} \in \mathcal{G}$ is then a convex combination of the current state g_i and of the atom \bar{g}_i . This convex combination depends on a step-size ρ_i which is pre-determined and different versions of the algorithm may have different step-size sequences.

Our goal in quadrature is to approximate the mean element μ_p . Recently [2] proposed to frame integration as a FW optimisation problem, with the domain $\mathcal{G} \subseteq \mathcal{H}$ being a space of functions and taking the objective function to be:

$$J(g) = \frac{1}{2} \|g - \mu_p\|^2. \quad (6)$$

Notice that when g is an approximation of the mean element, J takes the form of half the posterior variance (or the MMD^2) that is minimised in BQ. In the FW setting, minimisation of J is carried out over $\mathcal{G} = \mathcal{M}$, the marginal polytope of the RKHS \mathcal{H} . The marginal polytope \mathcal{M} is defined as the closure of the convex hull of $\Phi(\mathcal{X})$, so that in particular $\mu_p \in \mathcal{M}$. Assuming as in [17] that $\Phi(x)$ is uniformly bounded in feature space (i.e. $\exists R > 0 : \forall x \in \mathcal{X}, \|\Phi(x)\| \leq R$), then \mathcal{M} is a closed and bounded set and can be optimised over.

A particular advantage of this method is that it leads to ‘sparse’ solutions which are linear combinations of the atoms $\{\bar{g}_i\}_{i=1}^n$ [2]. In particular this provides a weighted estimate for the mean element:

$$\hat{\mu}_{\text{FW}} := g_n = \sum_{i=1}^n \left(\prod_{j=i}^{n-1} (1 - \rho_{j-1}) \rho_{i-1} \right) \bar{g}_i := \sum_{i=1}^n w_i^{\text{FW}} \bar{g}_i, \quad (7)$$

where by default $\rho_0 = 1$ which leads to all $w_i^{\text{FW}} \in [0, 1]$ when $\rho_i = 1/(i + 1)$. A typical sequence of approximations to the mean element is shown in Fig. 1 (left), demonstrating that the approximation quickly converges to the ground truth (in black). Since minimisation of a linear function can be restricted to extreme points of the domain, the atoms will be of the form $\bar{g}_i = \Phi(x_i^{\text{FW}}) = k(\cdot, x_i^{\text{FW}})$

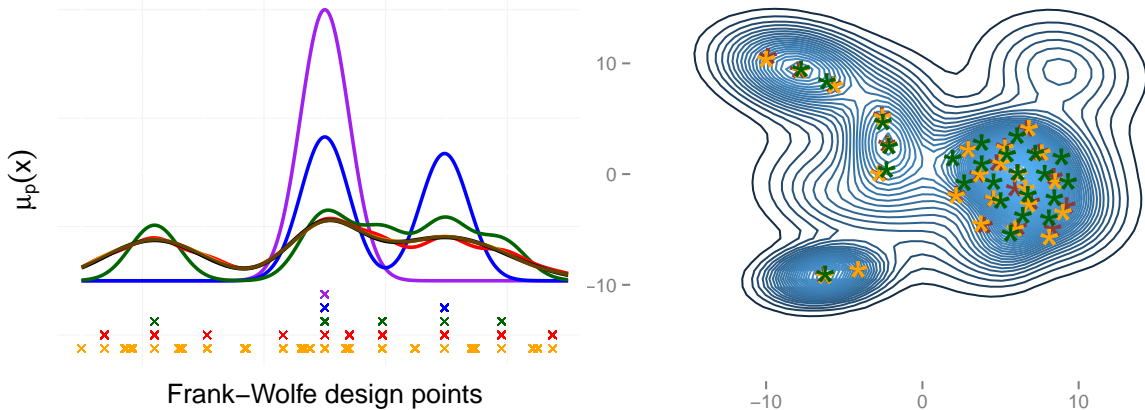


Figure 1: *Left*: Approximations to the mean element μ_p using the FWLS algorithm, based on $n = 1, 2, 5, 10, 50$ design points (purple, blue, green, red and orange respectively). It is not possible to distinguish between approximation and ground truth when $n = 50$. *Right*: Density of a mixture of 20 Gaussian distributions, displaying the first $n = 25$ design points chosen by FW (red), FWLS (orange) and SBQ (green). Each method provides well-spaced design points in high-density regions. Most FW and FWLS design points overlap, partly explaining their similar performance in this case.

for some $x_i^{\text{FW}} \in \mathcal{X}$. The minimisation in g over \mathcal{G} from step 2 in Algorithm 1 therefore becomes a minimisation in x over \mathcal{X} . In practice, at each iteration i , the FW algorithm hence selects a design point $x_i^{\text{FW}} \in \mathcal{X}$ which induces an atom \bar{g}_i and gives us an approximation of the mean element μ_p . We denote by $\hat{\mu}_{\text{FW}}$ this approximation after n iterations. Using the reproducing property, we can show that the FW estimate is a sigma-point rule:

$$\hat{p}_{\text{FW}}[f] := \langle f, \hat{\mu}_{\text{FW}} \rangle = \left\langle f, \sum_{i=1}^n w_i^{\text{FW}} \bar{g}_i \right\rangle = \sum_{i=1}^n w_i^{\text{FW}} \langle f, k(\cdot, x_i^{\text{FW}}) \rangle = \sum_{i=1}^n w_i^{\text{FW}} f(x_i^{\text{FW}}) \quad (8)$$

The total computational cost for FW is $\mathcal{O}(n^2)$ after n iterations. An extension known as FW with Line Search (FWLS) uses a line-search method to find the optimal step size ρ_i at each iteration (see Alg. 1). Once again, the approximation obtained after n steps of FWLS has a sparse expression as a convex combination of all the previously visited states and we obtain an associated sigma-point rule. FWLS has theoretical convergence rates that can be stronger than standard versions of the algorithm but has computational cost in $\mathcal{O}(n^3)$; we consider both approaches below. The authors in [9] provide a survey of FW-based algorithms and their convergence rates under different regularity conditions on the objective function and domain of optimisation.

Remark: The FW design points x_i^{FW} are generally not available in closed-form. We follow mainstream literature by selecting, at each iteration, the point that minimises the MMD over a finite collection of M points, drawn independently and at random from $p(x)$. [17] proved that this approximation adds a $\mathcal{O}(M^{-1/4})$ term to the MMD, so that theoretical results on FW convergence continue to apply provided that $M(n) \rightarrow \infty$ sufficiently quickly. Appendix A provides full details.

3 A Hybrid Approach: Frank-Wolfe Bayesian Quadrature

To combine the advantages of a probabilistic integrator with a formal convergence theory, we propose Frank-Wolfe Bayesian Quadrature (FWBQ). In FWBQ, design points $\{x_i^{\text{FW}}\}_{i=1}^n$ are selected by the FW algorithm. However, rather than combining these with the usual FW weights $\{w_i^{\text{FW}}\}_{i=1}^n$, we use instead the weights $\{w_i^{\text{BQ}}\}_{i=1}^n$ provided by BQ. Denote this sigma-point rule by \hat{p}_{FWBQ} . We also

consider FWLSBQ, which uses FWLS in place of FW. As we show below, these hybrid estimators (i) carry the Bayesian interpretation of Sec. 2.2, (ii) permit a rigorous theoretical analysis, and (iii) out-perform existing FW quadrature rules by orders of magnitude in simulations. FWBQ is hence ideally suited to probabilistic numerics applications.

For these theoretical results we assume that the test function f belongs to a finite-dimensional RKHS \mathcal{H} , in line with recent literature [2, 9, 16, 17]. We further assume that \mathcal{X} is a compact subset of \mathbb{R}^d , that $p(x) > 0$ for all $x \in \mathcal{X}$ and that the kernel k is continuous on $\mathcal{X} \times \mathcal{X}$. Under these hypotheses, Theorem 1 below establishes consistency of the posterior mean, while Theorem 2 establishes rates of contraction for the full posterior distribution. Write $a(n) \lesssim b(n)$ whenever $a(n)/b(n) = \mathcal{O}(1)$.

Theorem 1 (Consistency). *The posterior mean $\hat{p}_{\text{FWBQ}}[f]$ converges to the true integral $p[f]$ at the following rates:*

$$|p[f] - \hat{p}_{\text{FWBQ}}[f]| \lesssim \begin{cases} n^{-1} & \text{for FWBQ with step size } \rho_i = 1/(i+1) \\ \exp(-Cn) & \text{for FWLSBQ} \end{cases} \quad (9)$$

for some $0 < C < \infty$.

Proof. The posterior mean in BQ is a Bayes estimator and so the MMD takes a minimax form [15]. In particular, the BQ weights perform no worse than the FW weights:

$$\text{MMD}(\{x_i^{\text{FW}}, w_i^{\text{BQ}}\}_{i=1}^n) = \inf_{w \in \mathbb{R}^n} \text{MMD}(\{x_i^{\text{FW}}, w_i\}_{i=1}^n) \leq \text{MMD}(\{x_i^{\text{FW}}, w_i^{\text{FW}}\}_{i=1}^n). \quad (10)$$

Now, the values attained by the FW objective J along the path $\{g_i\}_{i=1}^n$ determined by the FW(/FWLS) algorithm can be expressed in terms of the MMD as follows:

$$J(g_n) = \frac{1}{2} \|\hat{\mu}_{\text{FW}} - \mu_p\|^2 = \frac{1}{2} \text{MMD}(\{x_i^{\text{FW}}, w_i^{\text{FW}}\}_{i=1}^n)^2. \quad (11)$$

Combining (10) and (11) gives

$$|p[f] - \hat{p}_{\text{FWBQ}}[f]| \leq \text{MMD}(\{x_i^{\text{FW}}, w_i^{\text{BQ}}\}_{i=1}^n) \|f\| \leq 2^{1/2} J(g_n)^{1/2} \|f\|. \quad (12)$$

To complete the proof we leverage recent analysis of the FW algorithm with steps $\rho_i = 1/(n+1)$ and the FWLS algorithm. Specifically, from [Prop. 1,[2]] we have that $\exists C_1, C_2 > 0$:

$$J(g_n) \leq \begin{cases} 2R^4/C_1^2 n^2 & \text{for FW} \\ R^2 \exp(-C_2^2 n/R^2) & \text{for FWLS} \end{cases} \quad (13)$$

where R is the diameter of the marginal polytope \mathcal{M} . \square

An immediate corollary of Theorem 1 is that FWLSBQ has an asymptotic error that is superior to that of any QMC estimator [6]. This is not a contradiction - recall that QMC restricts attention to uniform weights, while FWLSBQ is able to propose arbitrary weightings. In addition we highlight a robustness property: Even when the assumptions of this section do not hold, one still obtains at least a rate $\mathcal{O}_P(n^{-1/2})$ for the posterior mean using either FWBQ or FWLSBQ [7].

Remark: The choice of kernel affects the convergence of the FWBQ method [14]. Clearly, we expect faster convergence if the function we are integrating is ‘close’ to the space of functions induced by our kernel. Indeed, the kernel specifies the geometry of the marginal polytope \mathcal{M} , that in turn directly influences the rate constant R associated with FW convex optimisation.

Consistency is a stepping stone towards our main contribution, which establishes posterior contraction rates for FWBQ. Posterior contraction is important as these results justify, for the first time, the probabilistic numerics approach to integration; that is, we show that the *full* posterior distribution is a sensible quantification (at least asymptotically) of numerical error in the integration routine:

Theorem 2 (Contraction). *Let $S \subseteq \mathbb{R}$ be an open neighbourhood of the true integral $p[f]$. Then the posterior probability mass on $S^c = \mathbb{R} \setminus S$ vanishes at a rate:*

$$\text{prob}(S^c) \lesssim \begin{cases} n^{-1} \exp(-Cn^2) & \text{for FWBQ with step size } \rho_i = 1/(i+1) \\ \exp(-C_1 \exp(C_2 n)) & \text{for FWLSBQ} \end{cases} \quad (14)$$

for some $0 < C < \infty$ and $0 < C_1, C_2 < \infty$.

Proof. See Appendix B. □

Thus FWBQ enjoys both a probabilistic interpretation and rigorous theoretical guarantees. A notable corollary of our work is that OBQ enjoys the same rates of convergence and contraction, resolving a conjecture by Tony O’Hagan that OBQ converges exponentially [personal communication]:

Corollary. *The consistency and contraction rates obtained for FWLSBQ apply also to OBQ.*

Proof. By definition, OBQ chooses samples that globally minimise the MMD and we can hence bound this quantity from above by the MMD of FWLSBQ:

$$\text{MMD}(\{x_i^{\text{OBQ}}, w_i^{\text{BQ}}\}_{i=1}^n) = \inf_{x_1, \dots, x_n \in \mathcal{X}} \text{MMD}(\{x_i, w_i^{\text{BQ}}\}_{i=1}^n) \leq \text{MMD}(\{x_i^{\text{FW}}, w_i^{\text{BQ}}\}_{i=1}^n) \quad (15)$$

Consistency and contraction follow from inserting this inequality into the above proofs. □

4 Experimental Results

4.1 Simulation Study

To facilitate the experiments in this paper we followed [1, 2, 10, 17] and employed an exponentiated-quadratic (EQ) kernel $k(x, x') := \lambda^2 \exp(-1/2\sigma^2 \|x - x'\|^2)$. This corresponds to an infinite-dimensional RKHS, not covered by our theory; nevertheless, we note that all simulations are practically finite-dimensional due to rounding at machine precision. EQ kernels are popular in the BQ literature as, when p is a mixture of Gaussians, the mean element μ_p is analytically tractable (see Appendix C). Some other (p, k) pairs that produce analytic mean elements are discussed in [1].

For this simulation study, we took $p(x)$ to be a 20-component mixture of 2D-Gaussian distributions. Monte Carlo (MC) is often used for such distributions but has a slow convergence rate in $\mathcal{O}_P(n^{-1/2})$. FW and FWLS are known to converge more quickly and are in this sense preferable to MC [2]. In our simulations (Fig. 2, left), both our novel methods FWBQ and FWLSBQ decreased the MMD much faster than the FW/FWLS methods of [2]. Here, the same kernel hyper-parameters $(\lambda, \sigma) = (1, 0.8)$ were employed for all methods to have a fair comparison. This suggests that the best sigma-point rules correspond to elements *outside* the convex hull of $\{\Phi(x_i)\}_{i=1}^n$. Examples of those, including BQ, often assign negative weights to features (Fig. S1 right, Appendix D).

The principle advantage of our proposed methods is that they reconcile theoretical tractability with a fully probabilistic interpretation. For illustration, Fig. 2 (right) plots the posterior uncertainty due to numerical error for a typical integration problem based on this $p(x)$. In-depth empirical studies of such posteriors exist already in the literature and the reader is referred to [3, 12, 21] for details.

Beyond these theoretically tractable integrators, SBQ seems to give even better performance as the number of samples increases. An intuitive explanation is that SBQ picks design points to minimise the MMD whereas FWBQ and FWLSBQ only minimise an approximation to the MMD (its linearisation along the derivative DJ). In addition, the weights for SBQ are optimal at each iteration, which is not the case for FWBQ and FWLSBQ. We therefore conjecture that Theorem 1 and 2 should provide upper bounds on the rates of SBQ. This conjecture is partly supported by Fig. 1 (right), which shows that SBQ selects similar sets of design points to FW/FWLS (but weights them optimally). Note also that both FWBQ and FWLSBQ give very similar result. This is not so surprising as FWLS is not expected to converge exponentially in infinite-dimensional RKHS [16].

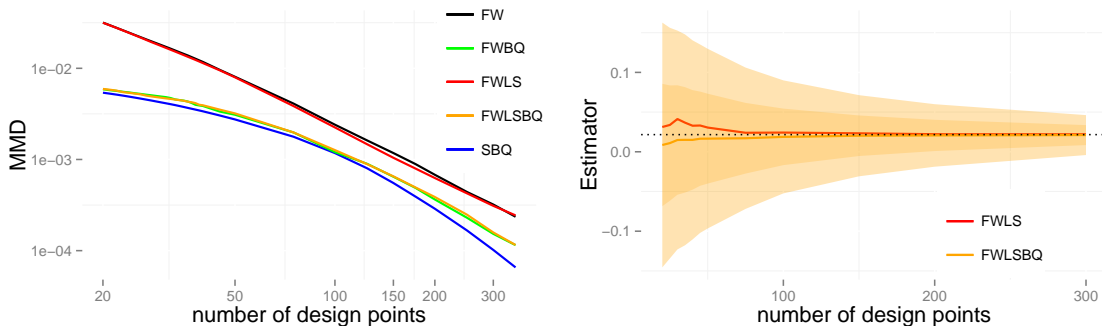


Figure 2: Simulation study. *Left*: Plot of the worst-case integration error (MMD). Both FWBQ and FWLSBQ are seen to outperform FW and FWLS, with SBQ performing best overall. *Right*: Integral estimates for FWLS and FWLSBQ for a function $f \in \mathcal{H}$. FWLS converges more slowly and provides only a point estimate for a given number of design points. In contrast, FWLSBQ converges faster and provides a full probability distribution over numerical error shown shaded in orange (68% and 95% credible intervals). Ground truth corresponds to the dotted black line.

4.2 Quantifying Numerical Error in a Proteomic Model Selection Problem

A topical bioinformatics application that extends recent work by [18] is presented. The objective is to select among a set $\{M_i\}_{i=1}^m$ of candidate models for protein regulation. This choice is based on a dataset \mathcal{D} of protein expression levels, in order to determine a ‘most plausible’ biological hypothesis for further experimental investigation. Each M_i is specified by a vector of kinetic parameters θ_i (full details in Appendix D). Bayesian model selection requires that these parameters are integrated out against a prior $p(\theta_i)$ to obtain marginal likelihood terms $L(M_i) = \int p(\mathcal{D}|\theta_i)p(\theta_i)d\theta_i$. Our focus here is on obtaining the *maximum a posteriori* (MAP) model M_j , defined as the maximiser of the posterior model probability $L(M_j)/\sum_{i=1}^m L(M_i)$ (where we have assumed a uniform prior over model space). Numerical error in the computation of each term $L(M_i)$, if unaccounted for, could cause us to return a model M_k that is different from the true MAP estimate M_j and lead to the mis-allocation of valuable experimental resources.

The problem is quickly exaggerated when the number m of models increases, as there are more opportunities for one of the $L(M_i)$ terms to be ‘too large’ due to numerical error. In [18], the number m of models was combinatorial in the number of protein kinases measured in a high-throughput assay (currently $\sim 10^2$ but in principle up to $\sim 10^4$). This led [18] to deploy substantial computing resources to ensure that numerical error in each estimate of $L(M_i)$ was individually controlled. Probabilistic numerics provides a more elegant and efficient solution: At any given stage, we have a fully probabilistic quantification of our uncertainty in each of the integrals $L(M_i)$, shown to be sensible both theoretically and empirically. This induces a full posterior distribution over numerical uncertainty in the location of the MAP estimate (i.e. ‘Bayes all the way down’). As such we can determine, on-line, the precise point in the computational pipeline when numerical uncertainty near the MAP estimate becomes acceptably small, and cease further computation.

The FWBQ methodology was applied to one of the model selection tasks in [18]. In Fig. 3 (left) we display posterior model probabilities for each of $m = 352$ candidates models, where a low number ($n = 10$) of design points were used to evaluate each integral. (For display clarity only the first 50 models are shown.) In this low- n regime, numerical error introduces a second level of uncertainty that we quantify by combining the FWBQ error models for all integrals in the computational pipeline; this is summarised by a box plot (rather than a single point) for each of the models (obtained by sampling - full details in Appendix D). These box plots reveal that our estimated posterior model probabilities are completely dominated by numerical error. In contrast, when n is increased through 50, 100 and

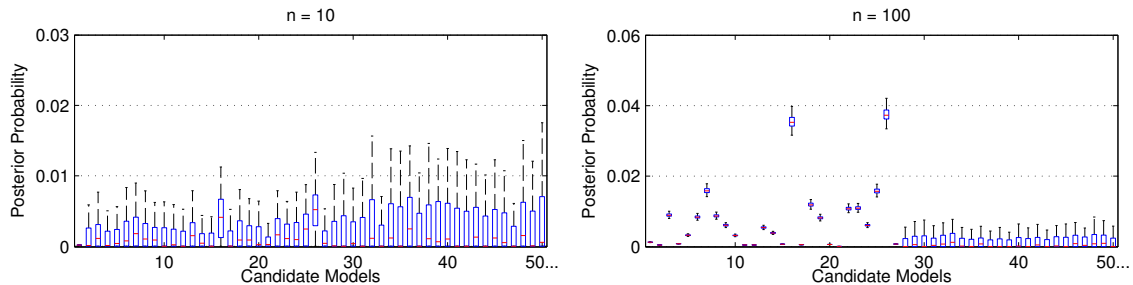


Figure 3: Quantifying numerical error in a model selection problem. FWBQ was used to model the numerical error of each integral $L(M_i)$ explicitly. For integration based on $n = 10$ design points, FWBQ tells us that the computational estimate of the model posterior will be dominated by numerical error (left). When instead $n = 100$ design points are used (right), uncertainty due to numerical error becomes much smaller (but not yet small enough to determine the MAP estimate).

200 (Fig. 3, right and Fig. S2), the uncertainty due to numerical error becomes negligible. At $n = 200$ we can conclude that model 26 is the true MAP estimate and further computations can be halted. Correctness of this result was confirmed using the more computationally intensive methods in [18].

In Appendix D we compared the relative performance of FWBQ, FWLSBQ and SBQ on this problem. Fig. S1 shows that the BQ weights reduced the MMD by orders of magnitude relative to FW and FWLS and that SBQ converged more quickly than both FWBQ and FWLSBQ.

5 Conclusions

This paper provides the first theoretical results for probabilistic approaches to integration, in the form of posterior contraction rates for the hybrid FWBQ and FWLSBQ methods. This is an important step in the probabilistic numerics research programme [14] as it establishes a theoretical justification for using the posterior distribution provided by BQ as a model for the numerical integration error (which was previously assumed by many authors [10, 11, 19, 22, 25]). The practical advantages conferred by a fully probabilistic error model were demonstrated on a model selection problem from cellular biology, where sensitivity of an evaluation of the MAP estimate was modelled as a function of the error arising from repeated numerical integration.

The strengths and weaknesses of BQ (notably, including scalability) are well-known and are inherited by our FWBQ methodology. We do not review these here but refer the reader to [21] for an extended discussion. Convergence, in the classical sense, was proven here to occur exponentially quickly for FWLSBQ, which partially explains the excellent performance of BQ and related methods seen in applications [11, 22], as well as resolving an open conjecture. As a bonus, the hybrid quadrature rules that we developed turned out to converge much faster in simulations than those in [2], which originally motivated our work.

A key open problem for kernel methods in probabilistic numerics is to establish protocols for the practical elicitation of kernel hyper-parameters. This is important as hyper-parameters directly affect the scale of the posterior over numerical error that we ultimately aim to interpret. Note that this problem applies equally to BQ, as well as related quadrature methods [2, 10, 11, 19] and more generally in probabilistic numerics [26]. Previous work, such as [12], optimised hyper-parameters on a per-application basis. Our ongoing research seeks automatic and general methods for hyper-parameter elicitation that provide good frequentist coverage properties for posterior credible intervals, but we reserve the details for a future publication.

Acknowledgments

The authors are grateful for discussions with Simon Lacoste-Julien, Simo Särkkä, Arno Solin, Tom Gunter and Mathias Cronjäger. FXB was supported by EPSRC [EP/L016710/1]. CJO was supported by EPSRC [EP/D002060/1]. MG was supported by EPSRC [EP/J016934/1], an EPSRC Established Career Fellowship, the EU grant [EU/259348] and a Royal Society Wolfson Research Merit Award.

References

- [1] F. Bach. On the Equivalence between Quadrature Rules and Random Features. *arXiv:1502.06800*, 2015.
- [2] F. Bach, S. Lacoste-Julien, and G. Obozinski. On the Equivalence between Herding and Conditional Gradient Algorithms. In *Proceedings of the 29th International Conference on Machine Learning*, 2012.
- [3] Y. Chen, L. Bornn, N. de Freitas, M. Eskelin, J. Fang, and M. Welling. Herded Gibbs Sampling. *Journal of Machine Learning Research*, 2015. To appear.
- [4] Y. Chen, M. Welling, and A. Smola. Super-Samples from Kernel Herding. In *Proceedings of the Conference on Uncertainty in Artificial Intelligence*, pages 109–116, 2010.
- [5] P. Diaconis. Bayesian Numerical Analysis. *Statistical Decision Theory and Related Topics IV*, 1988.
- [6] J. Dick and F. Pillichshammer. *Digital Nets and Sequences - Discrepancy Theory and Quasi-Monte Carlo Integration*. Cambridge University Press, 2010.
- [7] J. C. Dunn. Convergence Rates for Conditional Gradient Sequences Generated by Implicit Step Length Rules. *SIAM Journal on Control and Optimization*, 18(5):473–487, 1980.
- [8] M. Frank and P. Wolfe. An Algorithm for Quadratic Programming. *Naval Research Logistics Quarterly*, 3:95–110, 1956.
- [9] D. Garber and E. Hazan. Faster Rates for the Frank-Wolfe Method over Strongly-Convex Sets. In *Proceedings of the 32nd International Conference on Machine Learning*, 2015. To appear.
- [10] Z. Ghahramani and C. Rasmussen. Bayesian Monte Carlo. In *Advances in Neural Information Processing Systems*, pages 489–496, 2003.
- [11] T. Gunter, R. Garnett, M. Osborne, P. Hennig, and S. Roberts. Sampling for Inference in Probabilistic Models with Fast Bayesian Quadrature. In *Advances in Neural Information Processing Systems*, 2014.
- [12] J.B. Hamrick and T.L. Griffiths. Mental Rotation as Bayesian Quadrature. In *NIPS 2013 Workshop on Bayesian Optimization in Theory and Practice*, 2013.
- [13] P. Hennig. Probabilistic Interpretation of Linear Solvers. *SIAM Journal on Optimization*, 25:234–260, 2015.
- [14] P. Hennig, M. Osborne, and M. Girolami. Probabilistic Numerics and Uncertainty in Computations. *Proceedings of the Royal Society A*, 2015. To appear.
- [15] F. Huszar and D. Duvenaud. Optimally-Weighted Herding is Bayesian Quadrature. In *Uncertainty in Artificial Intelligence*, pages 377–385, 2012.
- [16] M. Jaggi. Revisiting Frank-Wolfe: Projection-Free Sparse Convex Optimization. *Proceedings of the 30th International Conference on Machine Learning*, 28:427–435, 2013.
- [17] S. Lacoste-Julien, F. Lindsten, and F. Bach. Sequential Kernel Herding : Frank-Wolfe Optimization for Particle Filtering. In *Proceedings of the 18th International Conference on Artificial Intelligence and Statistics*, pages 544–552, 2015.
- [18] C.J. Oates, F. Dondelinger, N. Bayani, J. Korkola, J.W. Gray, and S. Mukherjee. Causal Network Inference using Biochemical Kinetics. *Bioinformatics*, 30(17):i468–i474, 2014.
- [19] C.J. Oates, M. Girolami, and N. Chopin. Control Functionals for Monte Carlo Integration. *arXiv:1410.2392*, 2015.
- [20] A. O’Hagan. Monte Carlo is Fundamentally Unsound. *Journal of the Royal Statistical Society, Series D*, 36(2):247–249, 1984.
- [21] A. O’Hagan. Bayes-Hermite Quadrature. *Journal of Statistical Planning and Inference*, 29:245–260, 1991.

- [22] M. Osborne, R. Garnett, S. Roberts, C. Hart, S. Aigrain, and N. Gibson. Bayesian Quadrature for Ratios. In *Proceedings of the 15th International Conference on Artificial Intelligence and Statistics*, pages 832–840, 2012.
- [23] A.B. Owen. A Constraint on Extensible Quadrature Rules. *Numerische Mathematik*, 2015. To appear.
- [24] C. Rasmussen and C.K.I. Williams. *Gaussian Processes for Machine Learning*. MIT Press, 2006.
- [25] S. Sarkka, J. Hartikainen, L. Svensson, and F. Sandblom. On the Relation between Gaussian Process Quadratures and Sigma-Point Methods. *arXiv:1504.05994*, 2015.
- [26] M. Schober, D. Duvenaud, and P. Hennig. Probabilistic ODE solvers with Runge-Kutta means. In *Advances in Neural Information Processing Systems 25*, 2014.
- [27] B. Sriperumbudur, A. Gretton, K. Fukumizu, B. Schölkopf, and G. Lanckriet. Hilbert Space Embeddings and Metrics on Probability Measures. *Journal of Machine Learning Research*, 11:1517–1561, 2010.
- [28] R.A. Weinberg. *The Biology of Cancer*, volume 1. Garland Science, 2006.

Supplementary Material

Appendix A: Details for the FWBQ and FWLSBQ Algorithms

A high-level pseudo-code description for the Frank-Wolfe Bayesian Quadrature (FWBQ) algorithm is provided below.

Algorithm 2 The Frank-Wolfe Bayesian Quadrature (FWBQ) Algorithm

Require: function f , reproducing kernel k , initial point $x_0 \in \mathcal{X}$.

- 1: Compute design points $\{x_i^{\text{FW}}\}_{i=1}^n$ using the FW algorithm (Alg. 1).
 - 2: Compute associated weights $\{w_i^{\text{BQ}}\}_{i=1}^n$ using BQ (Eqn. 4).
 - 3: Compute the posterior mean $\hat{p}_{\text{FWBQ}}[f]$, i.e. the sigma-point rule with $\{x_i^{\text{FW}}, w_i^{\text{BQ}}\}_{i=1}^n$.
 - 4: Compute the posterior variance $v_{\text{BQ}}(\{x_i^{\text{FW}}\}_{i=1}^n)$ using BQ (Eqn. 5).
 - 5: Return the full posterior $\mathcal{N}(\hat{p}_{\text{FWBQ}}, v_{\text{BQ}}(\{x_i^{\text{FW}}\}_{i=1}^n))$ for the integral $p[f]$.
-

Frank-Wolfe Line-Search Bayesian Quadrature (FWLSBQ) is simply obtained by substituting the Frank-Wolfe algorithm with the Frank-Wolfe Line-Search algorithm. In this appendix, we derive expressions for the important steps in these algorithms that are required to implement them.

Expression to Compute the Minimisation of the Linearisation for the Frank-Wolfe and Frank-Wolfe Line-Search Algorithms (Step 3, Algorithm 1)

Let $w_i^{(n)}$ denote the weight assigned to x_i after n iterations of the FW algorithm. Below we obtain an equivalent expression of the minimisation of the linearisation of J in terms of kernel values and evaluations of the mean element at each iteration. Since minimisation of a linear function can be restricted to extreme points of the domain, we have that

$$\arg \min_{g \in \mathcal{G}} \langle g, (DJ)(g_n) \rangle = \arg \min_{x \in \mathcal{X}} \langle \Phi(x), (DJ)(g_n) \rangle.$$

Then using the definition of J we have

$$\arg \min_{x \in \mathcal{X}} \langle \Phi(x), (DJ)(g_n) \rangle = \arg \min_{x \in \mathcal{X}} \langle \Phi(x), g_n - \mu_p \rangle$$

where

$$\begin{aligned} \langle \Phi(x), g_n - \mu_p \rangle &= \langle \Phi(x), \sum_{i=1}^n w_i^{(n)} \Phi(x_i) - \mu_p \rangle \\ &= \sum_{i=1}^n w_i^{(n)} \langle \Phi(x), \Phi(x_i) \rangle - \langle \Phi(x), \mu_p \rangle \\ &= \sum_{i=1}^n w_i^{(n)} k(x, x_i) - \mu_p(x). \end{aligned}$$

Note that this expression may not be convex and may require us to make use of approximate methods to find the minimum x^* of this expression. To do so, we sample M points (where M is large) independently from the distribution p and pick the sample which minimises the expression above. From [17] this introduces an additive error term of size $\mathcal{O}(M^{-1/4})$, which does not impact our convergence analysis provided that $M(n)$ vanishes sufficiently quickly. In all experiments we took M between 10,000 and 50,000 so that this error will be negligible.

Expression to Compute the Line-Search Exactly for the Frank-Wolfe Line-Search Algorithm (Step 4, Algorithm 1)

Here we obtain an analytic expression for the line-search step in the FWLS. This expression will be given in terms of values of the kernel values and evaluations of the mean element.

First, from the definition of J

$$\begin{aligned}
J((1-\rho)g_n + \rho\Phi(x_{n+1})) &= \frac{1}{2} \langle (1-\rho)g_n + \rho\Phi(x_{n+1}) - \mu_p, (1-\rho)g_n + \rho\Phi(x_{n+1}) - \mu_p \rangle \\
&= \frac{1}{2} \left[(1-\rho)^2 \langle g_n, g_n \rangle + 2(1-\rho)\rho \langle g_n, \Phi(x_{n+1}) \rangle \right. \\
&\quad \left. + 2\rho^2 \langle \Phi(x_{n+1}), \Phi(x_{n+1}) \rangle - 2(1-\rho) \langle g_n, \mu_p \rangle \right. \\
&\quad \left. - 2\rho \langle \Phi(x_{n+1}), \mu_p \rangle + \langle \mu_p, \mu_p \rangle \right].
\end{aligned}$$

Taking the derivative of this expression with respect to ρ , we get:

$$\begin{aligned}
\frac{\partial J}{\partial \rho} &= \frac{1}{2} \left[-2(1-\rho) \langle g_n, g_n \rangle + 2(1-2\rho) \langle g_n, \Phi(x_{n+1}) \rangle \right. \\
&\quad \left. + 2\rho \langle \Phi(x_{n+1}), \Phi(x_{n+1}) \rangle + 2 \langle g_n, \mu_p \rangle - 2 \langle \Phi(x_{n+1}), \mu_p \rangle \right] \\
&= \rho \left[\langle g_n, g_n \rangle - 2 \langle g_n, \Phi(x_{n+1}) \rangle + \langle \Phi(x_{n+1}), \Phi(x_{n+1}) \rangle \right] \\
&= \rho \left\| g_n - \Phi(x_{n+1}) \right\|^2 - \langle g_n - \Phi(x_{n+1}), g_n - \mu_p \rangle.
\end{aligned}$$

Setting this derivative to zero gives us the following optimum:

$$\rho^* = \frac{\langle g_n - \mu_p, g_n - \Phi(x_{n+1}) \rangle}{\left\| g_n - \Phi(x_{n+1}) \right\|^2}.$$

Clearly, differentiating a second time with respect to ρ gives $\left\| g_n - \Phi(x_{n+1}) \right\|^2$, which is non-negative and so ρ^* is a minimum. One can show using geometrical arguments about the marginal polytope \mathcal{M} that ρ^* will be in $[0, 1]$ [16].

The numerator of this line-search expression is

$$\begin{aligned}
\langle g_n - \mu_p, g_n - \Phi(x_{n+1}) \rangle &= \langle g_n, g_n \rangle - \langle \mu_p, g_n \rangle - \sum_{i=1}^n w_i^{(n)} k(x_i, x_{n+1}) + \mu_p(x_{n+1}) \\
&= \sum_{i=1}^n \sum_{j=1}^n w_i^{(n)} w_j^{(n)} k(x_i, x_j) - \sum_{i=1}^n w_i^{(n)} \left[k(x_i, x_{n+1}) + \mu_p(x_i) \right] \\
&\quad + \mu_p(x_{n+1}).
\end{aligned}$$

Similarly the denominator is

$$\begin{aligned}
\left\| g_n - \Phi(x_{n+1}) \right\|^2 &= \langle g_n - \Phi(x_{n+1}), g_n - \Phi(x_{n+1}) \rangle \\
&= \langle g_n, g_n \rangle - 2 \langle g_n, \Phi(x_{n+1}) \rangle + \langle \Phi(x_{n+1}), \Phi(x_{n+1}) \rangle \\
&= \sum_{i=1}^n \sum_{j=1}^n w_i^{(n)} w_j^{(n)} k(x_i, x_j) - 2 \sum_{i=1}^n w_i^{(n)} k(x_i, x_{n+1}) + k(x_{n+1}, x_{n+1}).
\end{aligned}$$

Clearly all expressions provided here can be vectorised for efficient computational implementation.

Appendix B: Proof of Posterior Contraction

Theorem (Contraction). *Let $S \subseteq \mathbb{R}$ be an open neighbourhood of the true integral $p[f]$. Then the posterior probability mass on $S^c = \mathbb{R} \setminus S$ vanishes at a rate:*

$$\text{prob}(S^c) \lesssim \begin{cases} n^{-1} \exp(-Cn^2) & \text{for FWBQ with step size } \rho_i = 1/(i+1) \\ \exp(-C_1 \exp(C_2 n)) & \text{for FWLSBQ} \end{cases} \quad (16)$$

for some $0 < C < \infty$ or $0 < C_1, C_2 < \infty$.

Proof. We will obtain the posterior contraction rates of interest using the bounds on the MMD provided in the proof of Theorem 1. Given an open neighbourhood $S \subseteq \mathbb{R}$ of $p[f]$, we have that the complement $S^c = \mathbb{R} \setminus S$ is closed in \mathbb{R} . We assume without loss of generality that $S^c \neq \emptyset$, since the posterior mass on S^c is trivially zero when $S^c = \emptyset$. Since S^c is closed, the distance $D = \inf_{r \in S^c} |r - p[f]| > 0$ is strictly positive. Denote the posterior distribution by $\mathcal{N}(m_n, \sigma_n^2)$ where we have that $m_n := \hat{p}_{\text{FWBQ}}[f]$ where $\hat{p}_{\text{FWBQ}} = \sum_{i=1}^n w_i^{\text{BQ}} \delta(x_i^{\text{FW}})$ and $\sigma_n := \text{MMD}(\{x_i^{\text{FW}}, w_i^{\text{BQ}}\}_{i=1}^n)$. Directly from the supremum definition of the MMD we have:

$$|p[f] - m_n| \leq \sigma_n \|f\|. \quad (17)$$

Now the posterior probability mass on S^c is given by

$$M_n = \int_{S^c} \phi(r|m_n, \sigma_n) dr, \quad (18)$$

where $\phi(r|m_n, \sigma_n)$ is the p.d.f. of the posterior normal distribution. By the definition of D we get the upper bound:

$$M_n \leq \int_{-\infty}^{p[f]-D} \phi(r|m_n, \sigma_n) dr + \int_{p[f]+D}^{\infty} \phi(r|m_n, \sigma_n) dr \quad (19)$$

$$= 1 + \Phi\left(\underbrace{\frac{p[f] - m_n}{\sigma_n}}_{(*)} - \frac{D}{\sigma_n}\right) - \Phi\left(\underbrace{\frac{p[f] - m_n}{\sigma_n}}_{(*)} + \frac{D}{\sigma_n}\right). \quad (20)$$

From (17) we have that the terms $(*)$ are bounded by $\|f\| < \infty$ as $\sigma_n \rightarrow 0$, so that asymptotically we have:

$$M_n \lesssim 1 + \Phi(-D/\sigma_n) - \Phi(D/\sigma_n) \quad (21)$$

$$= \text{erfc}(D/\sqrt{2}\sigma_n) \sim (\sqrt{2}\sigma_n/\sqrt{\pi}D) \exp(-D^2/2\sigma_n^2). \quad (22)$$

Finally we may substitute the asymptotic results derived in the proof of Theorem 1 for the MMD σ_n into (22) to complete the proof. For FWBQ we have $\sigma_n \lesssim n^{-1}$, leading to $M_n \lesssim n^{-1} \exp(-Cn^2)$, whilst for FWLSBQ we have $\sigma \lesssim \exp(-Cn)$, leading to $M_n \lesssim \exp(-C_1 \exp(C_2 n))$. \square

Appendix C: Computing the Mean Element

We compute an expression for $\mu_p(x) = \int k(x, x') p(x') dx'$ in the case where k is an exponentiated-quadratic kernel with length scale hyper-parameter σ

$$k(x, x') := \lambda^2 \exp\left(\frac{-\sum_{i=1}^d (x_i - x'_i)^2}{2\sigma^2}\right) = \lambda^2 (\sqrt{2\pi}\sigma)^d \mathcal{N}(x|x', \Sigma_\sigma),$$

where Σ_σ is a d-dimensional diagonal matrix with entries σ^2 , and where $p(x)$ is a mixture of d-dimensional Gaussian distributions

$$p(x) = \sum_{l=1}^L \rho_l \phi(x|\mu_l, \Sigma_l).$$

(Note that, in this section only, x_i denotes the i th component of the vector x .) Using properties of Gaussian distributions (see Appendix A.2 of [24]) we obtain

$$\begin{aligned}
\mu_p(x) &= \int_{-\infty}^{\infty} k(x, x') p(x') dx' \\
&= \int_{-\infty}^{\infty} \lambda^2 (\sqrt{2\pi}\sigma)^d \phi(x'|x, \Sigma_\sigma) \times \left(\sum_{l=1}^L \rho_l \phi(x'|\mu_l, \Sigma_l) \right) dx' \\
&= \lambda^2 (\sqrt{2\pi}\sigma)^d \sum_{l=1}^L \rho_l \int_{-\infty}^{\infty} \phi(x'|x, \Sigma_\sigma) \times \phi(x'|\mu_l, \Sigma_l) dx' \\
&= \lambda^2 (\sqrt{2\pi}\sigma)^d \sum_{l=1}^L \rho_l \int_{-\infty}^{\infty} a_l^{-1} \phi(x'|c_l, C_l) dx' \\
&= \lambda^2 (\sqrt{2\pi}\sigma)^d \sum_{l=1}^L \rho_l a_l^{-1}.
\end{aligned}$$

where we have:

$$a_l^{-1} = (2\pi)^{-\frac{d}{2}} \left| \Sigma_\sigma + \Sigma_l \right|^{-\frac{1}{2}} \exp \left(-\frac{1}{2} (x - \mu_l)^T (\Sigma_\sigma + \Sigma_l)^{-1} (x - \mu_l) \right).$$

This last expression is in fact itself a Gaussian distribution with probability density function $\phi(x|\mu_l, \Sigma_l + \Sigma_\sigma)$ and we hence obtain:

$$\mu_p(x) := \lambda^2 (\sqrt{2\pi}\sigma)^d \sum_{l=1}^L \rho_l \phi(x|\mu_l, \Sigma_l + \Sigma_\sigma).$$

Finally, we once again use properties of Gaussians to obtain

$$\begin{aligned}
\int \mu_p(x) p(x) dx &= \int \left[\lambda^2 (\sqrt{2\pi}\sigma)^d \sum_{l=1}^L \rho_l \phi(x|\mu_l, \Sigma_l + \Sigma_\sigma) \right] \times \left[\sum_{m=1}^L \rho_m \phi(x|\mu_m, \Sigma_m) \right] dx \\
&= \lambda^2 (\sqrt{2\pi}\sigma)^d \sum_{l=1}^L \sum_{m=1}^L \rho_l \rho_m \int \phi(x|\mu_l, \Sigma_l + \Sigma_\sigma) \phi(x|\mu_m, \Sigma_m) dx \\
&= \lambda^2 (\sqrt{2\pi}\sigma)^d \sum_{l=1}^L \sum_{m=1}^L \rho_l \rho_m a_{lm}^{-1} \\
&= \lambda^2 (\sqrt{2\pi}\sigma)^d \sum_{l=1}^L \sum_{m=1}^L \rho_l \rho_m \phi(\mu_l|\mu_m, \Sigma_l + \Sigma_m + \Sigma_\sigma).
\end{aligned}$$

Other combinations of kernel k and density p that give rise to an analytic mean element can be found in the references of [1].

Appendix D: Application to Proteomics Data

Description of the Model Choice Problem

The ‘CheMA’ methodology described in [18] contains several elements that we do not attempt to reproduce in full here; in particular we do not attempt to provide a detailed motivation for the mathematical forms presented below, as this requires elements from molecular chemistry. For our present purposes it will be sufficient to define the statistical models $\{M_i\}_{i=1}^m$ and to clearly specify

the integration problems that are to be solved. We refer the reader to [18] and the accompanying supplementary materials for a full biological background.

Denote by \mathcal{D} the dataset containing normalised measured expression levels $y_S(t_j)$ and $y_S^*(t_j)$ for, respectively, the unphosphorylated and phosphorylated forms of a protein of interest ('substrate') in a longitudinal experiment at time t_j . In addition \mathcal{D} contains normalised measured expression levels $y_{E_i}^*(t_j)$ for a set of possible regulator kinases ('enzymes', here phosphorylated proteins) that we denote by $\{E_i\}$.

An important scientific goal is to identify the roles of enzymes (or 'kinases') in protein signaling; in this case the problem takes the form of variable selection and we are interested to discover which enzymes must be included in a model for regulation of the substrate S . Specifically, a candidate model M_i specifies which enzymes in the set $\{E_i\}$ are regulators of the substrate S , for example $M_3 = \{E_2, E_4\}$. Following [18] we consider models containing at most two enzymes, as well as the model containing no enzymes.

Given a dataset \mathcal{D} and model M_i , we can write down a likelihood function as follows:

$$L(\theta_i, M_i) = \prod_{n=1}^N \phi \left(\frac{y_S^*(t_{n+1}) - y_S^*(t_n)}{t_{n+1} - t_n} \left| -\frac{V_0 y_S^*(t_n)}{y_S^*(t_n) + K_0} + \sum_{E_j \in M_i} \frac{V_j y_{E_j}^*(t_n) y_S(t_n)}{y_S(t_n) + K_j}, \sigma^2 \right. \right). \quad (23)$$

Here the model parameters are $\theta_i = \{K, V, \sigma\}$, where $(K)_j = K_j$, $(V)_j = V_j$, ϕ is the normal p.d.f. and the mathematical forms arise from the Michaelis-Menten theory of enzyme kinetics. The V_j are known as 'maximum reaction rates' and the K_j are known as 'Michaelis-Menten parameters'. This is classical chemical notation, not to be confused with the kernel matrix from the main text. The final parameter σ defines the error magnitude for this 'approximate gradient-matching' statistical model.

The prior specification proposed in [18] and followed here is

$$K \sim \mathcal{N}_T(1, 2^{-1}\mathbf{I}), \quad (24)$$

$$\sigma|K \sim p(\sigma) \propto 1/\sigma, \quad (25)$$

$$V|K, \sigma \sim \mathcal{N}_T(1, N\sigma^2(\mathbf{X}(K)^T \mathbf{X}(K))^{-1}), \quad (26)$$

where \mathcal{N}_T denotes a Gaussian distribution, truncated so that its support is $[0, \infty)$ (since kinetic parameters cannot be non-negative). Here $\mathbf{X}(K)$ is the design matrix associated with the linear regression that is obtained by treating the K as known constants; we refer to [18] for further details.

Due to its careful design, the likelihood in Eqn. 23 is partially conjugate, so the following integral can be evaluated in closed form:

$$L(K, M_i) = \int \int L(\theta_i, M_i) p(V, \sigma|K) dV d\sigma. \quad (27)$$

The numerical challenge is then to compute the integral

$$L(M_i) = \int L(K, M_i) p(K) dK, \quad (28)$$

for each candidate model M_i . Depending on the number of enzymes in model M_i , this will either be a 1-, 2- or 3-dimensional numerical integral. Whilst such integrals are not challenging to compute on a per-individual basis, the nature of the application means that the values $L(M_i)$ will be similar for many candidate models and, when the number of models is large, this demands either a very precise calculation per model or a careful quantification of the impact of numerical error on the subsequent inferences (i.e. determining the MAP estimate). It is this particular issue that motivates the use of probabilistic numerical methods.

Description of the Computational Problem

We need to compute integrals of functions with domain $\mathcal{X} = [0, \infty)^d$ where $d \in \{1, 2, 3\}$ and the sampling distribution $p(x)$ takes the form $N_T(1, 2^{-1}\mathbf{I})$. The test function $f(x)$ corresponds to $L(\mathbf{K}, M_i)$ with $x = \mathbf{K}$. This is given explicitly by the g -prior formulae as:

$$L(\mathbf{K}, M_i) = \frac{1}{(2\pi)^{N/2}} \frac{1}{(N+1)^{d/2}} \Gamma\left(\frac{N}{2}\right) b_N^{-\frac{N}{2}}, \quad (29)$$

$$b_N = \frac{1}{2} \left(\mathbf{Y}^T \mathbf{Y} + \frac{1}{N} \mathbf{1}^T \mathbf{X}^T \mathbf{X} \mathbf{1} - \mathbf{V}_N^T \Omega_N \mathbf{V}_N \right), \quad (30)$$

$$\mathbf{V}_N = \Omega_N^{-1} \left(\frac{1}{N} \mathbf{X}^T \mathbf{X} \mathbf{1} + \mathbf{X}^T \mathbf{Y} \right) \quad (31)$$

$$\Omega_N = \left(1 + \frac{1}{N} \right) \mathbf{X}^T \mathbf{X} \quad (32)$$

$$(\mathbf{Y})_n = \frac{y_S^*(t_{n+1}) - y_S^*(t_n)}{t_{n+1} - t_n}, \quad (33)$$

$$(34)$$

where for clarity we have suppressed the dependence of \mathbf{X} on \mathbf{K} . For the Frank-Wolfe Bayesian Quadrature algorithm, we require that the mean element μ_p is analytically tractable and for this reason we employed the exponentiated-quadratic kernel with length scale λ and width scale σ parameters:

$$k(x, x') = \lambda^2 \exp\left(-\frac{\sum_{i=1}^d (x_i - x'_i)^2}{2\sigma^2}\right). \quad (35)$$

For simplicity we focussed on the single hyper-parameter pair $\lambda = \sigma = 1$, which produces:

$$\mu_p(x) = \int k(x, x') p(x') dx' \quad (36)$$

$$= \int \exp\left(-\sum_{i=1}^d (x_i - x'_i)^2\right) \phi_T(x' | 1, 2^{-1}\mathbf{I}) dx' \quad (37)$$

$$= 2^{-d/2} (1 + \operatorname{erf}(1))^{-d} \prod_{i=1}^d \exp\left(-\frac{(x_i - 1)^2}{2}\right) \left(1 + \operatorname{erf}\left(\frac{x_i + 1}{\sqrt{2}}\right)\right), \quad (38)$$

where ϕ_T is the p.d.f. of the truncated Gaussian distribution introduced above and erf is the error function. To compute the posterior variance of the numerical error we also require the quantity:

$$\int \int k(x, x') p(x) p(x') dx dx' = \int \mu_p(x) p(x) dx = \begin{cases} 0.629907\dots & \text{for } d = 1 \\ 0.396783\dots & \text{for } d = 2 \\ 0.249937\dots & \text{for } d = 3 \end{cases}, \quad (39)$$

which we have simply evaluated numerically. We emphasise that principled approaches to hyper-parameter elicitation are an important open research problem that we aim to address in a future publication (see discussion in the main text). The values used here are scientifically reasonable and serve to illustrate key aspects of our methodology.

FWBQ provides posterior distributions over the numerical uncertainty in each of our estimates for the marginal likelihoods $L(M_i)$. In order to propagate this uncertainty forward into a posterior distribution over posterior model probabilities (see Figs. 3 in the main text and S2 below), we simply sampled values $\hat{L}(M_i)$ from each of the posterior distributions for $L(M_i)$ and used these sample values to construct posterior model probabilities $\hat{L}(M_i) / \sum_j \hat{L}(M_j)$. Repeating this procedure many times enables us to sample from the posterior distribution over the posterior model probabilities (i.e. two levels of Bayes' theorem). This provides a principled quantification of the uncertainty due to numerical error in the output of our primary Bayesian analysis.

Description of the Data

The proteomic dataset \mathcal{D} that we considered here was a subset of the larger dataset provided in [18]. Specifically, the substrate S was the well-studied 4E-binding protein 1 (4EBP1) and the enzymes E_j consisted of a collection of key proteins that are thought to be connected with 4EBP1 regulation, or at least involved in similar regulatory processes within cellular signalling. Full details, including experimental protocols, data normalisation and the specific choice of measurement time points are provided in the supplementary materials associated with [18].

For this particular problem, biological interest arises because the data-generating system was provided by breast cancer cell lines. As such, the textbook description of 4EBP1 regulation may not be valid and indeed it is thought that 4EBP1 dis-regulation is a major contributing factor to these complex diseases (see [28]). We do not elaborate further on the scientific rationale for model-based proteomics in this work.

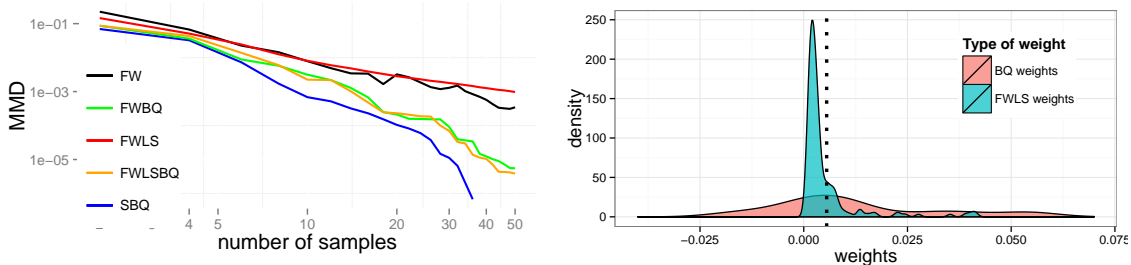


Figure S1: Comparison of quadrature methods on the proteomics dataset. *Left*: Value of the MMD for FW (black), FWLS (red), FWBQ (green), FWLSBQ (orange) and SBQ (blue). Once again, we see the clear improvement of using Bayesian Quadrature weights and we see that Sequential Bayesian Quadrature improves on Frank-Wolfe Bayesian Quadrature and Frank-Wolfe Line-Search Bayesian Quadrature. *Right*: Empirical distribution of weights. The dotted line represent the weights of the Frank-Wolfe algorithm with line search, which has all weights $w_i = 1/n$. Note that the distribution of Bayesian Quadrature weights ranges from -17.39 to 13.75 whereas all versions of Frank-Wolfe have weights limited to $[0, 1]$ and have to sum to 1.

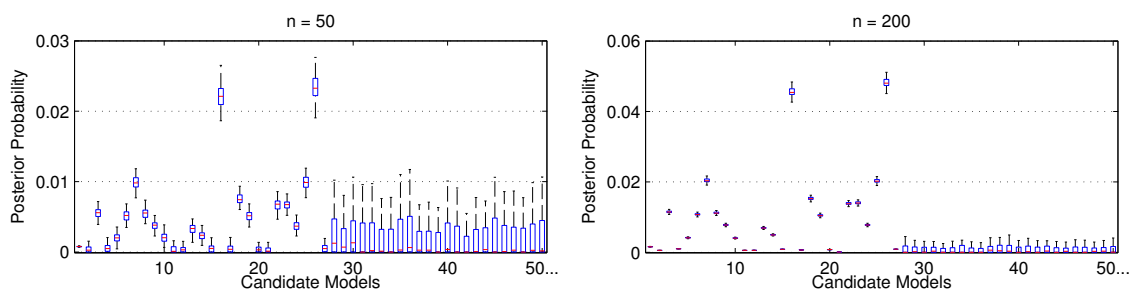


Figure S2: Quantifying numerical error in a model selection problem. Marginalisation of model parameters necessitates numerical integration and any error in this computation will introduce error into the reported posterior distribution over models. Here FWBQ is used to model this numerical error explicitly. *Left*: At $n = 50$ design points the uncertainty due to numerical error prevents us from determining the true MAP estimate. *Right*: At $n = 200$ design points, models 16 and 26 can be better distinguished as the uncertainty due to numerical error is reduced (model 26 can be seen to be the MAP estimate, although some uncertainty about this still remains even at this value of n , due to numerical error).